Structure of the Mesophotic Macroalgal Communities from Offshore Hard Banks in Louisiana before and after the 2010 Deepwater Horizon Oil Spill

Dagoberto E Venera-Pontón*, William E Schmidt, Suzanne Fredericq

Department of Biology, University of Louisiana at Lafayette, Lafayette LA 70506-3602, USA

ABSTRACT

The mesophotic macroalgal communities offshore Louisiana, NW Gulf of Mexico are exceptionally biodiverse on hard banks located at 50-100 m depth. Despite their vulnerability to oil spills, little is known about the seasonal and spatial dynamics of these algal communities after the 2010 Deepwater Horizon oil spill (DWH). This study addresses this deficiency by compiling data on macroalgal abundances from 14 research cruises that sampled two offshore banks near the vicinity of the DWH Macondo oil well blowout. Statistical analyses revealed a strong seasonal structure in which environmental changes were followed by community changes after a month. This delayed response was linked to *in situ* temperatures, coinciding with various studies worldwide reporting temperature as the main predictor of seasonal structure in macroalgal communities. Additionally, this study provides evidence that the DWH may have affected the macroalgal community of Ewing Bank. Summer box dredges launched after the DWH lacked several macroalgal taxa that before the disaster were typically associated with that season; nonetheless, Summer dredges post-DWH showed a greater biodiversity due to the presence of other macroalgae. This biodiversity rise resembled a temporary response rather than a permanent outcome since the increase was statistically significant only during 2011, and seems to have progressively declined towards pre-DWH levels. Conversely, macroalgal composition seems to be progressively diverging from pre-DWH conditions. Importantly, community changes post-DWH are not necessarily caused by spilled oil but may be a consequence of other factors associated with the event.

Keywords: Community ecology; Disturbance; Macondo oil spill; Marine pollution; Gulf of Mexico; Seasonality; Seaweeds; Temperature

INTRODUCTION

Offshore hard banks in the NW Gulf of Mexico (GoMx) harbor rich mesophotic macroalgal communities comprised of hundreds of species with broad morphological diversity [1-3]; such biodiversity contrasts with the GoMx's coastal ecosystems, which are dominated by mixed turfs or extensive mats (< 1 cm in height) of small cryptic forms [2,4-7]. In Louisiana, these offshore banks are typically salt domes formed when thick mineral beds, mainly halite, intruded vertically into the rocky marine substrata, creating elevations known as diapirs [8,9]. The taxonomic diversity of macroalgae associated with these salt domes has been extensively described [2,10,11].

In addition to their macroalgal diversity, salt domes are important for the oil industry because they are associated with petroleum deposits [9,12,13]; consequently, their biological communities are typically near numerous oil rigs and may be especially vulnerable to oil spills. Despite their high biodiversity and vulnerability, little is known about their seasonal and spatial dynamics, patterns of species dominance, or their community structure in general. This gap in knowledge is an important limitation for understanding the impacts of human and natural disturbances due to the lack of a baseline that can be compared with ecological assessments of a disturbance event.

This limitation became particularly important after the 2010 Deepwater Horizon oil spill (DWH), considered the largest marine oil spill in U.S. history [14-17]. This disaster started on April 2010 with the Macondo well explosion (28° 44.29' N, 88° 21.96' W) and lasted 87 days, during which 780,000 m³ of crude oil was leaked in the GoMx along with 7,000 m³ of Corexit oil dispersant [18-21]. Due to the lack of quantitative data, the DWH impact on offshore macroalgal communities was mostly evaluated by qualitatively

comparing the presence/absence of species before and after the disaster [10,22]. Such an approach, although relevant, may produce misleading conclusions if, for example, typical seasonal dynamics are wrongly attributed to the disaster. The existence of this possibility, consequently, highlights the need of quantitative assessments that clarify the typical dynamics of the macroalgal community.

This study addressed this problem with a retrospective approach, reconstructing the macroalgal abundances on two Louisiana offshore banks (located near the DWH explosion) from their frequencies of occurrence in Hourglass-design box dredges launched during multiple research cruises conducted before and after the DWH [23]. Based on these data and other environmental factors, this study evaluated: 1) the seasonal and site-specific dynamics of two macroalgal communities associated with offshore banks; 2) the environmental drivers of the community; and 3) the potential effects of the DWH disaster.

MATERIALS AND METHODS

Study area

This study evaluated two hard banks offshore Louisiana, NW Gulf of Mexico, that have been the focus of phycological investigations by our research group since 1998 [2] and were exposed to the DWH [10,22,24-30]. The dynamic structure of the macroalgal communities inhabiting Ewing Bank (28° 8.06' N, 90° 54.63' W) and Sackett Bank (28° 36.17' N, 89° 33.02' W) was reconstructed from the records of 14 research cruises made during 2000-2014 (Table 1). Hourglass-design box dredges were dragged for a period of ≤10 minutes on the bottom with the ship moving against the current/wind [23]. Samples were identified using morphological characters compiled from resources listed in Fredericq et al. [2]. The macroalgal diversity of each sample was based on two functional group (F-group) systems, referred to hereafter as Semi-Taxa and Balata Groups. The latter follow the system of Balata et al. which considers 11 groups of Chlorophyta, 12 groups of Ochrophyta, and 12 of Rhodophyta [31]. Conversely, the Semi-Taxa approach used the genera (or families) originally recorded [3].

Dredges with zero macroalgae were not excluded because doing so would hamper the power of multivariate analyses to detect potential consequences of disturbances such as the DWH. For example, mass die-offs or strong decreases in macroalgal abundance would be hardly detected if empty dredges were excluded [32,33]. Nevertheless, the distribution of dredging depths was carefully examined for each location using Box and Whisker plots: dredges deeper than the median by more than 1.5 interquartile ranges (IQRs) were considered outliers and excluded.

The occurrence (presence/absence) of F-groups was used to evaluate patterns of similarity between dredges whereas the F-group abundances were used to evaluate patterns of similarity between cruises. Bray-Curtis Matrices of Similarity (BC matrix) were built for each location and examined with multivariate statistical analyses [33,34,35]. To prevent divisions by zero in the empty dredges, Bray-Curtis calculations were zero-adjusted by adding a dummy F-group with abundance = 1 in all the dredges [33,36]. For Semi-Taxa, abundances were defined as the percent frequency of occurrence in dredges; conversely, Balata Group abundances were defined as their number of Semi-Taxa per dredge.

A set of monthly mean fields for temperature, salinity, dissolved oxygen (O_2), apparent oxygen utilization, percent oxygen saturation, phosphate, silicate, and nitrate was obtained from the NOAA National Center for Environmental Information and used to build Euclidean Matrices of Environmental Distance (ED Matrices) between dredges and cruises. The fields are part of the World Ocean Atlas 2013 (version 2) and cover the entire GoMx at a horizontal resolution of one degree and a vertical resolution of 5 m for depths ≤100 m. The fields represent central tendencies for all the records available in the World Ocean Database for the time span between 1955 and 2012 [37]. ED matrices were examined with multivariate statistical analyses along with the biological data.

Multivariate statistical analyses

Non-Metric Multidimensional Scaling (nMDS) and Unconstrained Divisive Clustering (UNCTREE) were used to evaluate the similarity patterns between dredges/cruises in the BC and ED matrices [33,36], and the extent to which they support the existence of: distinct communities at each location; seasonal changes in community structure; and DWH-associated changes in community

Table 1: Dredges launched at Ewing and Sackett banks during each of 14 research cruises that are referenced by date. Ewing Bank was sampled for all the cruises while Sackett Bank was sampled for nine of the cruises.

Cruise	Ewing Dredges	Depth (m)	Sackett Dredges	Depth (m)
May 2000	6	58-60	-	-
June-July 2001	5	~72.5	-	-
July 2003 (GoMx LA)	13	51.5-97	-	-
May-June 2004 (NSF I)	3	55.5-63	3	66-68.95
June 2005 (NSF II)	4	57-87	-	-
June-July 2006 (NSF III)	6	55-100	7	63-66.3
August 2008 (NW GoM)	16	53.5-85.5	9	59.85-70.5
December 2010 (NSF IV)	10	54.5-85.6	3	59-61
April 2011 (NSF V RAPID)	7	55.5-97	4	61-64
August 2011 (GRI-I)	10	54.5-105	6	63.08-76.25
August 2012 (GoMRI)	4	53.5-56.5	4	72-92.5
November 2012 (GoMRI)	3	56-66.5	-	-
October 2013 (GoMRI)	8	56.5-87.5	3	62.5-72
September 2014 (GoMRI)	3	58-59	5	65-66.5

structure. The UNCTREE dendrograms were further examined with Tests of Similarity Profiles (SIMPROF) to determine which clusters have significant multivariate structure and can be safely interpreted [38].

To determine whether the environmental factors satisfactorily explain the local dynamics in the macroalgal communities from Ewing and Sackett banks, the BC and ED matrices were examined with Constrained Divisive Clustering [38] and BIOENV analyses [39]. LINKTREEs were also used to find the F-group subsets that best explain the community dynamics [33,36].

Analyses of Similarity (ANOSIMs) were used to determine whether Ewing and Sackett bank show statistically significant differences in the dynamics of their macroalgal communities. Likewise, ANOSIMs were used to determine whether the macroalgal communities from each location show statistically significant differences between seasons and, importantly, before vs. after the DWH. Abundance-based ANOSIMs were integrated in a 3-Way fully crossed design [33,36] that included seasons (Spring, Summer, and Fall), locations (Ewing and Sackett), and the DWH (before vs. after) as factors. This design allowed the evaluation of each factor without ignoring the potential effect of the others. Conversely, Dredge-based ANOSIMs used a One-Way design that evaluated DWH-associated patterns within particular seasons and locations. Whenever statistically significant differences were found, Similarity Percentage Breakdowns (SIMPERs) were used to determine which F-groups contribute most to the dissimilarity [33,36].

The environmental variables were normalized to a common scale where the mean equals zero and the standard deviation equals one. The association and data distribution between environmental variables were evaluated in Draftsman Plots and a Matrix of Correlations before normalization. A detailed description of all the multivariate methods is provided in Legendre & Legendre, Clarke et al. and Clarke & Gorley [33,35,36].

Univariate comparisons of diversity and dominance

The macroalgal diversity, defined as the number of F-groups per dredge, was compared between locations (Ewing vs. Sackett bank), seasons (e.g. Spring vs. Fall), and before vs. after the DWH. These comparisons were performed with Analyses of Variance (ANOVAs) and T-tests whenever the macroalgal diversities met the parametric assumptions of homoscedasticity and normality [35,40] which were tested with Shapiro-Wilks', Levene's, Bartlett's, and Cochran's tests. Whenever the parametric assumptions were not met, the comparisons were produced with Kruskal-Wallis tests. Parametric post-hoc analyses were conducted with Tukey-Kramer tests whereas non-parametric post-hoc analyses were performed with Wilcoxon tests [35,40]. The dominance structure was also compared between locations (Ewing vs. Sackett bank), seasons (e.g. Spring vs. Fall), and before vs. after the DWH. These comparisons were based on cruise-specific plots of cumulative dominance, which were used as replicates in a DOMDIS matrix of distance and further analyzed with 3-Way fully-crossed ANOSIMs [33,36].

RESULTS

Seasonal dynamics and the Deepwater Horizon oil spill

Abundance-based UNCTREEs and nMDSs showed a strong seasonal structure at Ewing Bank: cruises from April-July grouped together and are referred to hereafter as the spring cluster; cruises from August-September formed a Summer cluster; and cruises from October-November formed a Fall cluster (Figure 1). Interestingly, the only cruise from December fell in the summer cluster. These seasonal clusters were supported by SIMPROF tests (P-Values <0.05) in both F-group approaches, except the fall cluster in Semi-Taxa. None of the nodes in the Sackett Bank UNCTREEs (abundance-based) were SIMPROF-supported (P-Value >0.05), regardless of the F-group approach; therefore, the seasonal structure of Sackett Bank could not be examined with ordination methods.
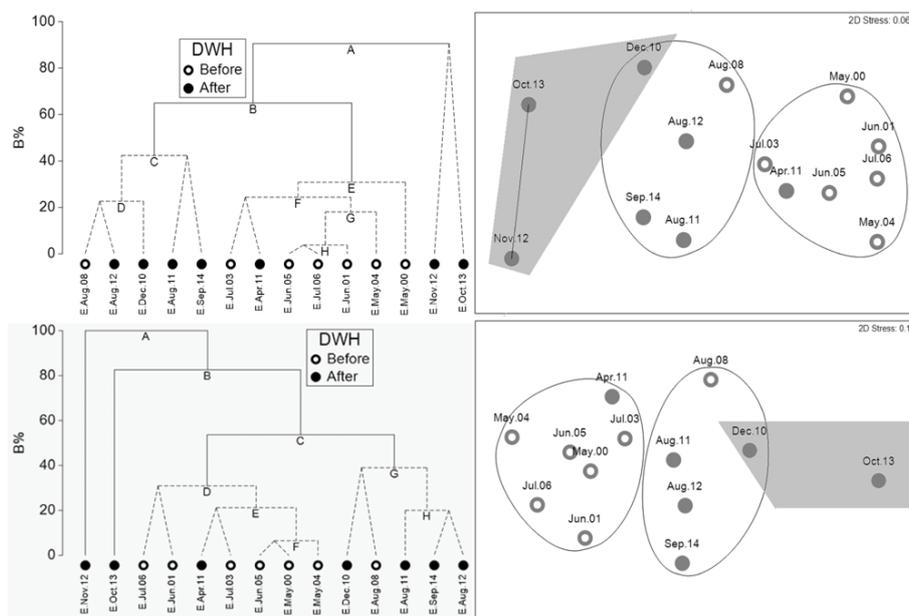
Figure 1: Unconstrained Divisive Clusters (UNCTREE; at left) and Non-Metric Multidimensional Scaling plots (nMDS; at right) showing the pattern of similarity between cruise samples collected during 2000-2014 in Ewing Bank. Each dot represents a cruise-specific set of F-Group abundances, labeled with the collection date (month.year). White and dark dots represent samples collected before vs. after the Deepwater Horizon oil spill, respectively. Nodes located on UNCTREE's solid lines are supported by Tests of Similarity Profiles (SIMPROF P-Values <0.05) whereas nodes located on dashed lines are not. SIMPROF-supported groups are also indicated in the nMDS plots with ovals or lines. Shaded zones indicate seasonal groups that were not clearly detected in the UNCTREE but are somewhat supported in the nMDS plot. The top-plots used Balata Groups whereas bottom-plots used Semi-Taxa.

Alternatively, Sackett Bank nMDS plots showed a relatively weak seasonal structure in both F-group approaches with cruises from April-June vs. August-December occupying opposite sides of the plots (Figure 2).

The patterns of similarity between cruises, as observed in UNCTREEs and nMDS plots, did not appear affected by the DWH disaster for either of the locations or F-group approaches (Figures 1,2). Instead, it appeared as if any dissimilarity between cruises from before vs. after the DWH can be solely explained by seasonality. 3-Way ANOSIMs, based on Balata Groups, further confirmed that seasonality is the main factor affecting the macroalgal community structure (R-Value = 0.616), followed by locations (0.555), whereas the DWH did not show a statistically significant effect (P-Value >0.05 and R-Value <0.3) (Table 2). Conversely, 3-Way ANOSIMs based on Semi-Taxa showed locations as the main community driver. The potential effect of the DWH was further evaluated with dredge-based BC matrices on separate analysis for each season. Dredge-based One-Way ANOSIMs and nMDS found that the summer community of Ewing Bank changed after the DWH whereas Sackett Bank and the spring assemblages did not show statistically significant differences associated to this event (Table 3, Figure 3).

Contributions of F-groups and environmental factors to the seasonal and DWH-associated dynamics

LINKTREEs, built an explained with F-group abundances of Ewing bank, produced the same dendrograms as their corresponding UNCTREEs (Figure 1). The dissimilarity between summer and Spring cruises was explained with the largest abundances of hollow red thalli (e.g. *Champia*, *Scinaia*), *Botryocladia*, and large corticated

Table 2: Multifactor Analyses of Similarity performed on the Matrices of Bray-Curtis similarity between cruises. Seasons, locations, and the Deepwater Horizon oil spill (DWH; before vs. after) were included as fully crossed factors. Seasons were based on the Unconstrained Divisive Clusters of Ewing Bank. The P-Values for Season and Location are based on 999 permutations whereas the DWH P-Value is based on 336. Global R-Values were interpreted as follows: <0.2: no differences, ≥0.2: little differences, ≥0.3: moderate, ≥0.5: strong, ≥0.7 very strong.

Factor	Balata Groups		Semi-Taxa	
	Global-R	P-Value	Global-R	P-Value
Season	0.616	0.004	0.445	0.045
Location	0.555	0.014	0.692	0.003
DWH	0.25	0.214	0.274	0.193
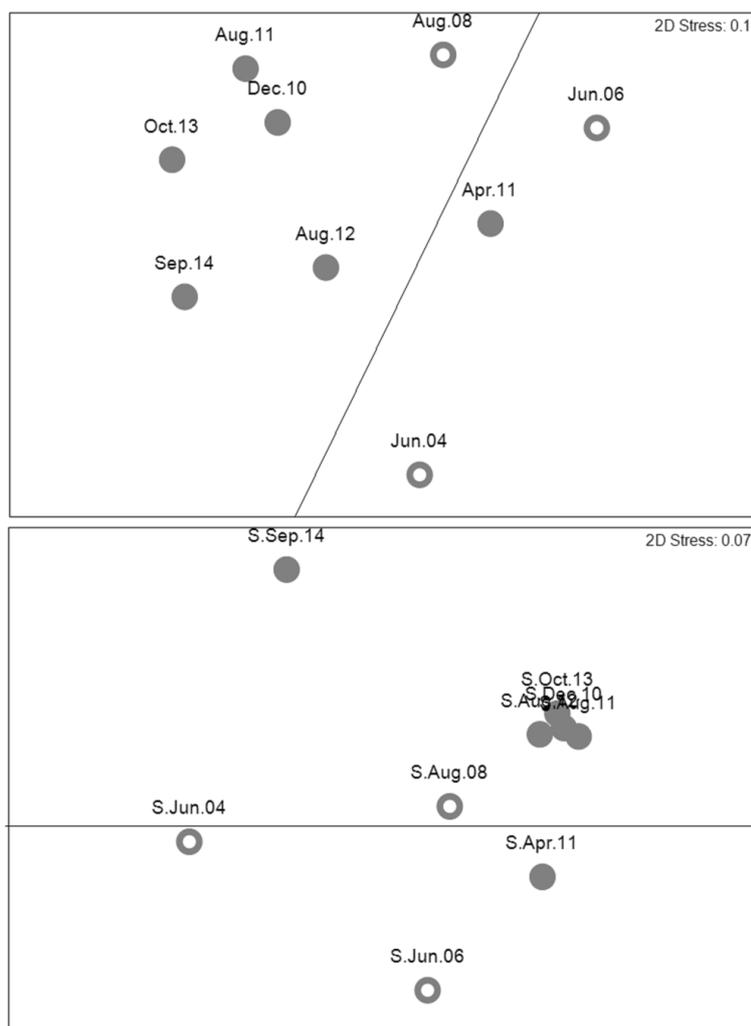
Figure 2: Non-Metric Multidimensional Scaling plots showing the pattern of similarity between cruise samples collected during 2004-2014 at Sackett bank. Each dot represents a cruise-specific set of macroalgal abundances, labeled with the collection date (month.year). White and dark dots represent samples collected before vs. after the Deepwater Horizon oil spill, respectively. The line in the middle of the plots separates samples collected in April-June from samples collected in August-December. The top-plot is based on Balata Groups whereas the bottom-plot is based on Semi-Taxa.

Table 3: One-Way Analyses of Similarity (ANOSIM) performed on the Matrices of Bray-Curtis similarity between dredges. Each ANOSIM compared the dredges launched before vs. after the Deepwater Horizon oil spill within a particular season and location. Seasons were based on the Unconstrained Divisive Clusters of Ewing Bank and the P-Values were based on 999 permutations. R-Values were interpreted as follows: <0.2: no differences, ≥0.2: little differences, ≥0.3: moderate, ≥0.5: strong, ≥0.7 very strong.

Location-Season	Balata Groups		Semi-Taxa	
	R-Value	P-Value	R-Value	P-Value
Ewing-Summer	0.3	0.001	0.410	0.001
Ewing-Spring	-0.104	0.678	-0.009	0.499
Sackett-Summer	0.236	0.046	0.063	0.155
Sackett-Spring	-0.138	0.765	0.136	0.145
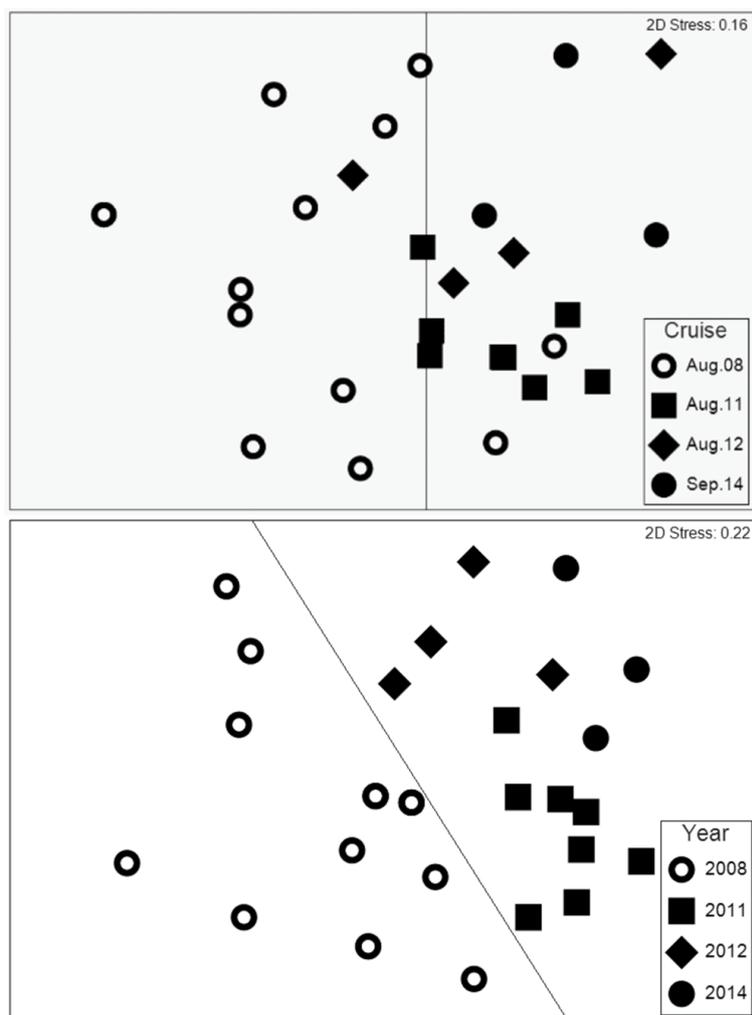
Figure 3: Multidimensional Scaling plots showing the pattern of similarity between Summer dredges at Ewing Bank. The top-plot used Balata Groups whereas the bottom-plot used Semi-Taxa. The line in the plot separate dredges launched before (white circles) vs. after (black shapes) the Deepwater Horizon oil spill (DWH). Dredges from different years are represented with different shapes. The DWH-associated patterns observed in these plots were more demarcated in the 3D plots (not shown) which had stress values of 0.1 for Balata Groups and 0.14 for Semi-Taxa.

Rhodophyta (e.g. *Gracilaria*, *Hypnea*, *Gelidium*) during the Spring. The dissimilarity between Fall and other seasons was linked to the lowest abundances (during Fall) of flattened macrophyta (e.g. *Halymenia*, *Kallymenia*) and large corticated Rhodophyta, which showed intermediate abundances during Summer.

The percent contributions of Balata Groups and Semi-Taxa to the pairwise dissimilarities between seasons at Ewing bank are shown in the SIMPERs of Table 4 and Table 5. Likewise, the contributions to dissimilarity between cruise-samples collected before vs. after the DWH at Ewing Bank are indicated in Table 6 whereas the contributions to dissimilarity between Ewing and Sackett banks are indicated in Table 7.

LINKTREEs, with environmental factors as explanatory variables, explained the biological dissimilarity between spring and summer with the lower *in situ* temperatures during the Spring (Figure 4). Likewise, the biological dissimilarity between fall and other seasons was explained with the largest surface percent oxygen saturation (0 m depth), lowest nitrate (5 m depth and vertical average) and silicate (5-30 m depth and vertical average) concentrations, salinity (30 m depth), and higher *in situ* temperatures, during the fall. A BIOENV analysis of the Balata BC Matrix of Ewing Bank, with environmental factors as explanatory variables, confirmed that the seasonal dynamics of the macroalgal community is strongly correlated with *in situ* temperature (correlation = 0.532); such

Table 4: Similarity Percentage Breakdowns indicating the percent contribution (Contrib%) of Balata Groups to the pairwise dissimilarities between seasons at Ewing bank. Only the most influential F-groups, whose contributions add to at least 70%, are shown. The seasonal average abundances are indicated in the columns labeled with the corresponding season. Av.Diss: average dissimilarity; Diss/SD: dissimilarity divided by the standard deviation; Cum.%: cumulative percent contribution.

Balata Group	Spring	Summer	Av.Diss	Diss/SD	Contrib%	Cum.%
LargeCorticated.R	2.2212	0.5449	8.86	2.16	14.89	14.89
FlattenedMacrophyta.R	1.8370	0.6330	7.00	1.35	11.78	26.67
HollowThallus.R	1.2898	0.1338	6.42	1.40	10.80	37.47
SmallCorticated.R	1.2377	0.1394	6.02	2.02	10.12	47.59
EncrustingCalcified.R	0.4275	1.3405	5.76	1.42	9.68	57.26
Postrate.R	0.6420	1.3958	4.71	1.12	7.92	65.18
CompressedBlade.B	0.5578	0.6378	2.76	1.03	4.64	69.82
BladeLike.C	0.6149	0.2885	2.36	1.73	3.96	73.78
Balata Group	**Spring**	**Fall**	**Av.Diss**	**Diss/SD**	**Contrib%**	**Cum.%**
LargeCorticated.R	2.2212	0.1845	13.95	2.90	17.36	17.36
FlattenedMacrophyta.R	1.8370	0.1845	11.33	1.51	14.09	31.44
HollowThallus.R	1.2898	0.0000	9.20	1.57	11.44	42.88
SmallCorticated.R	1.2377	0.0000	8.67	2.13	10.78	53.66
EncrustingCalcified.R	0.4275	1.2599	6.31	1.16	7.85	61.51
BladeLike.C	0.6149	0.0000	4.44	3.12	5.52	67.03
CompressedBranched.B	0.5950	0.0000	4.11	2.28	5.11	72.14
Balata Group	**Summer**	**Fall**	**Av.Diss**	**Diss/SD**	**Contrib%**	**Cum.%**
EncrustingCalcified.R	1.3405	1.2599	11.36	1.18	18.61	18.61
Postrate.R	1.3958	0.3909	11.27	1.36	18.46	37.08
CompressedBlade.B	0.6378	0.1310	5.95	1.81	9.74	46.82
FlattenedMacrophyte.R	0.6330	0.1845	5.51	1.88	9.04	55.85
LargeCorticated.R	0.5449	0.1845	4.83	1.23	7.92	63.77
CodiumErect.C	0.3926	0.0000	4.36	2.02	7.15	70.92

correlation was slightly lower than the best combinations of environmental factors (correlations <0.65). Conversely, when the same BIOENV analysis was applied to Semi-Taxa, the seasonal dynamics showed the strongest correlation (0.511) with surface percent oxygen saturation than *in situ* temperature (correlation = 0.403).

An nMDS plot (Figure 4), performed on the ED matrix for Ewing Bank, found differences between the seasonal structures of the environmental factors and the macroalgal communities. For example, the environmental conditions of summer started in July (Figure 4) but the macroalgal community did not show statistically significant changes until August (Figure 1). Moreover, whereas the environmental conditions of summer ended in September, the macroalgal community did not show statistically significant changes until October. This delay in the response of the macroalgal community to the overall environmental changes coincides with a delay in the peak of maximum *in situ* temperature, compared with the peak of surface temperature (Figure 4).

Seasonal patterns of biodiversity and the DWH

Macroalgal diversity, measured as the number of F-groups per dredge (GpD), did not show statistically significant differences between cruises at Sackett Bank, regardless of the annual season or whether the collection occurred before vs. after the DWH. A 2-Way Analysis of Variances (ANOVAs) showed P-Values >0.05 for seasons, DWH, and factor interactions in Sackett Bank; similarly, P-Values >0.05 were found in the Kruskal-Wallis test, with Cruises

as the factor. In contrast, Cruises from Ewing Bank showed a strong seasonal pattern (Kruskal-Wallis P-Value <0.05; Figure 5, Table 8). This pattern was further supported by a 2-Way ANOVA (P-Values <0.05 for Seasons) and post-hoc Tukey-Kramer tests (P-Values <0.05 for all the pairwise comparisons between seasons; Figure 5: bottom-left). Dredges launched during the spring showed the largest macroalgal diversity (11.86 GpD), followed by summer dredges (6.55 GpD) and, lastly, Fall dredges (2.31 GpD).

Interestingly, the 2-Way ANOVA showed P-Values >0.05 for DWH but <0.05 for the DWH*Seasons interaction; further examinations of this interaction in the Cruises' Wilcoxon tests (Table 8) showed a DWH-associated effect in the summer cruises (Figure 5: bottom-right) but no effect in the spring cruises. During the summer of 2008, before the DWH, the macroalgal diversity was 4.54 GpD; then, during August 2011, the first summer after the DWH, the macroalgal diversity increased to 9.75 GpD. In August 2012, the summer diversity decreased again (6.38 GpD) and remained relatively stable until 2014 (7 GpD). Only the dredges of August 2011 showed statistically significant differences with summer dredges from other years (Wilcoxon test P-Values <0.05; Table 8; Figure 6: bottom-right).

Finally, the dominance structure of the macroalgal community, analyzed with 3-Way ANOSIMs of the DOMDIS matrix, was significantly affected by locations and seasons but unaffected by the DWH (Table 9, Figure 6). The effects of locations and seasons were very strong on Balata Groups (P-Values <0.05 and R-Values >0.7); conversely, the dominance structure of Semi-Taxa was strongly

affected by locations (P-Value <0.05; R-Value >0.501) but weakly affected by seasons (P-Value <0.05; R-Value <0.3). This low Global R-Value, however, contrasted with the pairwise R-Value of 0.45 for the differences in Semi-Taxa dominance between fall and spring. Nevertheless, in both locations, the community experienced the largest dominance during the fall, followed by the summer, whereas the Spring showed the lowest dominance. Likewise, on each season, the community from Sackett Bank experienced greater dominance than that of Ewing Bank.

DISCUSSION

Seasonal changes in temperature and the macroalgal community

All the statistical analyses, without exceptions, supported the existence of a strong seasonal structure in the macroalgal communities from offshore Louisiana. From April to July (Spring), the community showed the highest abundances of hollow red thalli, flattened macrophyta, *Botryocladia*, and large-corticated Rhodophyta in general; this annual period also showed the largest biodiversity

and lowest dominance (Figure 5,6). Likewise, from August to September (summer), the community showed intermediate biodiversity and dominance, as well as intermediate abundances of flattened macrophyta and large corticated Rhodophyta. These F-groups showed their lowest abundances during October and November but re-gained intermediate abundances during December. The intermediate abundances of flattened macrophyta and large corticated Rhodophyta during December explain this month's similarity with the summer communities.

Seasonal changes of the macroalgal community were linked and strongly correlated to changes of *in situ* temperatures (see LINKTREEs and BIOENV analyses). This coincided with previous studies on the coastal communities from Texas and Louisiana [5,6], supporting the role of temperature as an essential driver of macroalgal communities in the NW Gulf of Mexico (GoMx). Temperature, among other parameters, has been extensively reported as a key predictor of seasonal macroalgal structure in a wide range of ecosystems that include tropical coastal habitats as well as temperate and arctic latitudes [41-44].

Table 5: Similarity Percentage Breakdowns indicating the percent contribution (Contrib%) of Semi-Taxa to the pairwise dissimilarities between seasons at Ewing bank. Only the most influential Semi-Taxa, whose contributions add to at least 70%, are shown. The seasonal average abundances are indicated in the columns labeled with the corresponding season. Av.Diss: average dissimilarity; Diss/SD: dissimilarity divided by the standard deviation; Cum.%: cumulative percent contribution.

Semi-Taxa	Summer	Fall	Av.Diss	Diss/SD	Contrib%	Cum.%
Peyssonnelia.R	69.39	23.21	9.71	1.48	12.06	12.06
Stypopodium.B	41.67	4.17	7.16	1.01	8.89	20.95
Codium.C	37.34	0.00	6.64	1.46	8.24	29.19
Halymenia.R	38.54	4.17	6.38	1.43	7.92	37.11
Coralline.R	35.42	23.21	5.58	1.19	6.93	44.03
Dictyota.B	21.55	0.00	3.95	2.23	4.90	48.94
Rhodymeniaceae.R	18.99	4.76	3.40	0.98	4.22	53.15
Cryptonemia.R	18.43	9.52	3.14	1.25	3.90	57.05
Valonia.C	17.71	0.00	3.08	1.22	3.82	60.88
Botryocladia.R	17.07	4.76	2.96	1.07	3.68	64.55
Lobophora.B	10.10	13.69	2.25	1.28	2.79	67.34
Scinaia.R	11.46	0.00	2.08	0.76	2.59	69.93
Microdictyon.C	12.50	0.00	2.08	0.54	2.58	72.51
Struvea.C	12.50	0.00	2.04	0.93	2.53	75.04
Semi-Taxa	**Summer**	**Spring**	**Av.Diss**	**Diss/SD**	**Contrib%**	**Cum.%**
Botryocladia.R	17.07	70.65	3.75	2.52	5.49	5.49
Chrysymenia.R	0.00	48.90	3.53	1.34	5.18	10.67
Stypopodium.B	41.67	7.73	2.88	1.07	4.23	14.89
Dictyota.B	21.55	55.93	2.44	1.36	3.58	18.47
Dasya.R	1.92	35.43	2.42	1.33	3.55	22.02
Halymenia.R	38.54	58.18	2.39	1.45	3.50	25.52
Microdictyon.C	12.50	32.94	2.33	1.24	3.42	28.93
Coelarthrum.R	0.00	31.15	2.28	1.29	3.34	32.28
Codium.C	37.34	25.48	2.02	1.24	2.96	35.24
Coralline.R	35.42	21.97	1.98	1.34	2.90	38.14
Peyssonnelia.R	69.39	55.76	1.82	1.28	2.66	40.80
Predaea.R	2.88	26.52	1.78	1.00	2.61	43.41
Titanophora.R	0.00	24.39	1.66	1.60	2.43	45.84
Sporochnus.B	0.00	23.81	1.52	0.74	2.23	48.07
Platoma.R	9.13	21.75	1.51	0.85	2.21	50.29

Cryptonemia.R	18.43	15.71	1.39	1.31	2.03	52.32
Cladophora.C	8.17	19.52	1.38	0.84	2.02	54.34
Padina.B	8.89	21.59	1.32	1.30	1.93	56.27
Lobophora.B	10.10	12.01	1.30	0.80	1.90	58.17
Gracilaria.R	6.25	18.92	1.28	1.13	1.87	60.04
Valonia.C	17.71	17.12	1.27	1.31	1.86	61.91
Wrightiella.R	0.00	19.03	1.23	1.03	1.80	63.71
Rhodymeniaceae.R	18.99	14.16	1.22	1.20	1.79	65.49
Scinaia.R	11.46	19.52	1.18	1.24	1.73	67.22
Delesseriaceae.R	3.13	17.84	1.16	1.40	1.69	68.92
Kallymenia.R	1.92	15.48	1.15	0.82	1.69	70.60
Semi-Taxa	**Fall**	**Spring**	**Av.Diss**	**Diss/SD**	**Contrib%**	**Cum.%**
Botryocladia.R	4.76	70.65	6.20	2.82	6.97	6.97
Dictyota.B	0.00	55.93	5.02	2.09	5.64	12.62
Halymenia.R	4.17	58.18	4.75	2.14	5.34	17.96
Chrysymenia.R	0.00	48.90	4.72	1.28	5.31	23.27
Peyssonnelia.R	23.21	55.76	3.69	1.44	4.15	27.42
Dasya.R	0.00	35.43	3.29	1.28	3.70	31.12
Microdictyon.C	0.00	32.94	3.19	1.14	3.59	34.70
Coelarthrum.R	0.00	31.15	3.06	1.24	3.45	38.15
Coralline.R	23.21	21.97	2.47	1.26	2.78	40.93
Predaea.R	0.00	26.52	2.42	0.96	2.72	43.64
Titanophora.R	0.00	24.39	2.18	1.57	2.45	46.09
Codium.C	0.00	25.48	2.16	1.05	2.43	48.52
Padina.B	0.00	21.59	2.05	1.22	2.31	50.82
Sporochnus.B	0.00	23.81	1.95	0.73	2.19	53.01
Platoma.R	0.00	21.75	1.88	0.72	2.12	55.13
Lobophora.B	13.69	12.01	1.85	0.87	2.08	57.21
Cladophora.C	4.76	19.52	1.78	0.75	2.00	59.21
Scinaia.R	0.00	19.52	1.74	1.27	1.95	61.16
Gracilaria.R	0.00	18.92	1.60	0.98	1.80	62.96
Wrightiella.R	0.00	19.03	1.59	1.03	1.79	64.75
Kallymenia.R	4.76	15.48	1.57	0.82	1.77	66.51
Valonia.C	0.00	17.12	1.56	0.93	1.75	68.26
Anadyomene.C	0.00	16.88	1.49	1.02	1.67	69.94
Cryptonemia.R	9.52	15.71	1.48	0.91	1.67	71.61

Table 6: Similarity Percentage Breakdowns indicating the percent contribution (Contrib%) of F-groups to the dissimilarity between cruise-samples collected before vs. after the Deepwater Horizon Oil Spill (DWH) at Ewing bank. Only the most influential Semi-Taxa, whose contributions add to at least 70%, are shown. The average abundances before vs. after the DWH are indicated. Av.Diss: average dissimilarity; Diss/SD: dissimilarity divided by the standard deviation; Cum.%: cumulative percent contribution.

Semi-Taxa	Before	After	Av.Diss	Diss/SD	Contrib%	Cum.%
Anadyomene.C	1.00	0.00	2.81	7.13	4.30	4.30
Asteromenia.R	1.00	0.00	2.81	7.13	4.30	8.60
Calonitophyllum.R	1.00	0.00	2.81	7.13	4.30	12.90
Champia.R	1.00	0.00	2.81	7.13	4.30	17.21
Coralline.R	0.00	1.00	2.81	7.13	4.30	21.51
Dasya.R	1.00	0.00	2.81	7.13	4.30	25.81
Halymenia.R	0.00	1.00	2.81	7.13	4.30	30.11
Kallymenia.R	1.00	0.00	2.81	7.13	4.30	34.41
Lithophyllum.R	1.00	0.00	2.81	7.13	4.30	38.71
Lithothamnion.R	1.00	0.00	2.81	7.13	4.30	43.01
Phyllodictyon.C	1.00	0.00	2.81	7.13	4.30	47.31
Predaea.R	1.00	0.00	2.81	7.13	4.30	51.62

	Before	After	Av.Diss	Diss/SD	Contrib%	Cum%
Pseudocodium.C	1.00	0.00	2.81	7.13	4.30	55.92
Rhodymenia.R	1.00	0.00	2.81	7.13	4.30	60.22
Valonia.C	0.00	1.00	2.81	7.13	4.30	64.52
Cladophora.C	1.00	0.33	2.00	1.15	3.06	67.58
Lobophora.B	1.00	0.33	2.00	1.15	3.06	70.64
Padina.B	1.00	0.33	2.00	1.15	3.06	73.70
Stypopodium.B	0.00	0.67	2.00	1.15	3.06	76.75
Platoma.R	1.00	0.33	1.89	1.12	2.89	79.64
Scinaia.R	0.00	0.67	1.89	1.12	2.89	82.53
Struvea.C	0.00	0.67	1.74	1.15	2.66	85.18
Botryocladia.R	1.00	0.67	1.08	0.58	1.64	86.83
Rhodymeniaceae.R	1.00	0.67	1.08	0.58	1.64	88.47
Neogoniolithon.R	0.00	0.33	0.93	0.58	1.42	89.89
Rhizophyllis.R	0.00	0.33	0.93	0.58	1.42	91.30
Cryptonemia.R	1.00	0.67	0.81	0.58	1.24	92.54
Delesseriaceae.R	0.00	0.33	0.81	0.58	1.24	93.79
Dictyopteris.B	0.00	0.33	0.81	0.58	1.24	95.03
Balata Group	**Before**	**After**	**Av.Diss**	**Diss/SD**	**Contrib%**	**Cum%**
Encrusting.B	1.00	0.00	4.07	12.26	16.52	16.52
SiphonousVesicle.C	0.00	1.00	4.07	12.26	16.52	33.04
BladeLike.R	1.00	0.33	2.84	1.15	11.51	44.56
CodiumCrust.C	0.00	0.67	2.84	1.15	11.51	56.07
FilamentousUniseriate.C	1.00	0.33	2.84	1.15	11.51	67.58
SmallCorticated.R	1.00	0.33	2.68	1.14	10.89	78.47
BladeLike.C	1.00	0.67	1.45	0.58	5.88	84.35
HollowThallus.R	1.00	0.67	1.39	0.58	5.63	89.98
FilamentousErect.R	0.00	0.33	1.23	0.58	5.01	94.99
LeatheryMacrophyte.B	0.00	0.33	1.23	0.58	5.01	100.00

Table 7: Similarity Percentage Breakdowns indicating the percent contribution (Contrib%) of F-Groups to the dissimilarity between locations during each season. Only the most influential F-groups, whose contributions add to at least 70%, are shown. The local average abundances are indicated in the rows labeled with the corresponding location. Av.Diss: average dissimilarity; Diss/SD: dissimilarity divided by the standard deviation; Cum.%: cumulative percent contribution.

Season	Balata Group	Ewing	Sackett	Av.Diss	Diss/SD	Contrib%	Cum.%
	LargeCorticated	2.2212	1.1786	8.02	1.21	13.95	13.95
	HollowThallus	1.2898	0.00	7.42	1.49	12.9	26.86
	FlattenedMacrophyte	1837	1.0159	7.31	1.26	12.72	39.57
	SmallCorticated	1.2377	0.2857	5.89	1.51	10.25	49.83
Spring	CompressedBlade	0.5578	0.2857	3.46	0.97	6.02	55.84
	BladeLike.R	0.3673	0.8571	3.45	1.74	6.01	61.85
	Postrate	0.642	0.7381	3.26	1.5	5.67	67.52
	EncrustingCalcified	0.4275	0.754	3.06	1.48	5.32	72.84
	Balata Group	**Ewing**	**Sackett**	**Av.Diss**	**Diss/SD**	**Contrib%**	**Cum.%**
	EncrustingCalcified	1.3405	0.7986	10.31	1.37	16.71	16.71
	Postrate	1.3958	0.7708	8.16	1.21	13.23	29.95
	CompressedBlade	0.6378	0.00	6.94	2.39	11.25	41.2
Summer	BladeLike.R	0.113	0.6875	6.36	1.35	10.32	51.52
	FlattenedMacrophyte	0.633	0.1667	5.22	2.04	8.46	59.98
	LargeCorticated	0.5449	0.3264	4.37	1.46	7.08	67.06
	CodiumErect	0.3926	0.00	4.02	2.03	6.52	73.57
	Semi-Taxa	**Ewing**	**Sackett**	**Av.Diss**	**Diss/SD**	**Contrib%**	**Cum.%**

	Semi-Taxa	Ewing	Sackett	Av.Diss	Diss/SD	Contrib%	Cum.%
Spring	Chrysymenia.R	48.9	0	3.57	1.27	4.68	4.68
	Botryocladia.R	70.65	29.76	3.56	1.38	4.67	9.35
	Dictyota.B	55.93	8.33	3.4	1.57	4.46	13.81
	Peyssonnelia.R	55.76	52.38	2.86	1.38	3.76	17.57
	Halymenia.R	58.18	30.95	2.72	1.35	3.57	21.14
	Struvea.C	5.95	43.25	2.57	1.72	3.37	24.51
	Cryptonemia.R	15.71	45.63	2.53	1.57	3.33	27.84
	Dasya.R	35.43	0	2.51	1.24	3.29	31.13
	Coelarthrum.R	31.15	0	2.3	1.22	3.02	34.16
	Coralline.R	21.97	25	2.29	1.27	3	37.16
	Rhodymenia.R	15.45	39.29	2.26	1.43	2.97	40.13
	Microdictyon.C	32.94	9.52	2.05	0.93	2.69	42.81
	Predaea.R	26.52	14.29	1.96	1.13	2.58	45.39
	Lobophora.B	12.01	23.81	1.93	0.8	2.53	47.92
	Codium.C	25.48	0	1.68	1.04	2.21	50.13
	Titanophora.R	24.39	0	1.67	1.52	2.2	52.33
	Sporochnus.B	23.81	4.76	1.6	0.83	2.1	54.43
	Padina.B	21.59	0	1.56	1.18	2.04	56.47
	Platoma.R	21.75	9.52	1.55	0.81	2.04	58.51
	Delesseriaceae.R	17.84	37.3	1.46	1.62	1.92	60.44
	Cladophora.C	19.52	0	1.39	0.72	1.82	62.26
	Scinaia.R	19.52	0	1.34	1.27	1.76	64.01
	Gracilaria.R	18.92	8.33	1.29	1.11	1.69	65.71
	Wrightiella.R	19.03	0	1.24	1	1.62	67.33
	Valonia.C	17.12	0	1.19	0.89	1.56	68.89
	Kallymenia.R	15.48	0	1.14	0.72	1.5	70.39
	Semi-Taxa	**Ewing**	**Sackett**	**Av.Diss**	**Diss/SD**	**Contrib%**	**Cum.%**
Summer	Stypopodium.B	41.67	0	5.83	0.95	7.8	7.8
	Halymenia.R	38.54	0	5.46	1.46	7.3	15.1
	Codium.C	37.34	0	5.39	1.56	7.21	22.31
	Coralline.R	35.42	36.11	4.78	1.21	6.39	28.7
	Peyssonnelia.R	69.39	54.86	4.27	1.42	5.72	34.42
	Dictyota.B	21.55	0	3.18	2.54	4.26	38.67
	Delesseriaceae.R	3.13	21.53	2.76	1.85	3.69	42.36
	Rhodymeniaceae.R	18.99	2.78	2.72	1.14	3.64	46
	Rhodymenia.R	1.92	17.36	2.63	0.99	3.51	49.51
	Botryocladia.R	17.07	0	2.59	1.27	3.47	52.98
	Valonia.C	17.71	0	2.52	1.3	3.36	56.35
	Cryptonemia.R	18.43	16.67	2.48	1.32	3.32	59.67
	Mesophyllum.R	0	12.5	1.87	0.55	2.5	62.17
	Sebdenia.R	0	12.5	1.87	0.55	2.5	64.67
	Microdictyon.C	12.5	0	1.71	0.56	2.29	66.96
	Scinaia.R	11.46	0	1.69	0.79	2.26	69.21
	Struvea.C	12.5	0	1.69	0.97	2.25	71.47
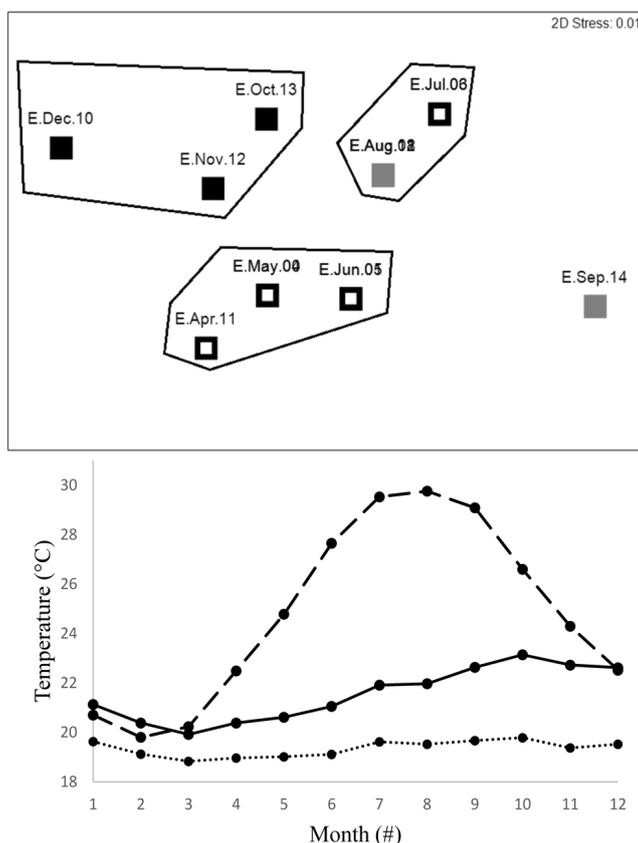
Figure 4: Seasonal changes in the environmental conditions at Ewing Bank. The Non-Metric Multidimensional Scaling plot (top) shows the environmental similarity between cruise samples collected at different annual seasons during 15 years. This analysis used an Euclidean Matrix of Distances built with multiple environmental factors. The seasonal structure of the macroalgal community, based on the Unconstrained Divisive Clusters of Ewing Bank, is also indicated with the square colors. White: Spring; Gray: Summer; Black: Fall. Cruises with similar environmental conditions are indicated with polygons. The bottom-chart shows the monthly changes of temperature in the ocean surface (5 m depth; dashed line), *in situ* (65 m depth; solid line), and at 100 m depth (dotted line). Both charts were built with mean fields obtained from the World Ocean Atlas 2013 (version 2) database.
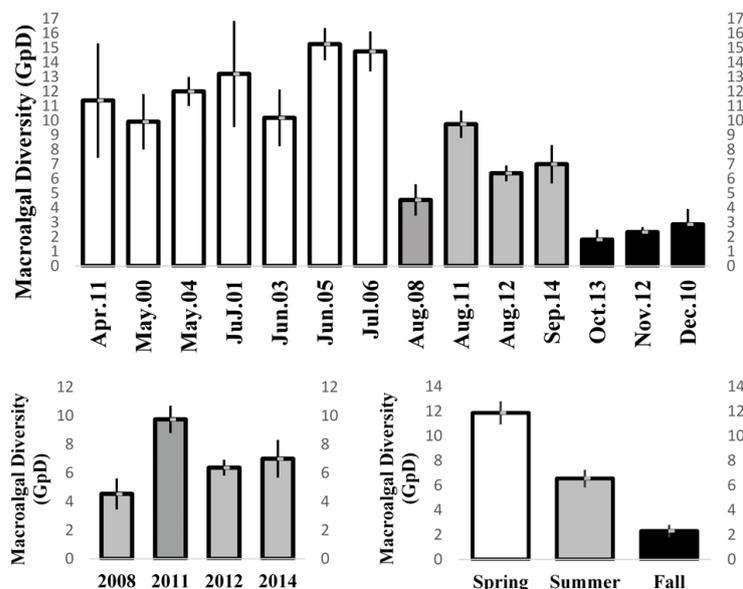
Figure 5: Patterns of macroalgal diversity, measured as the number of F-groups per dredge (GpD), at Ewing Bank. Bars represent the average GpD ± SE. The top chart presents 14 research cruises, sorted by month and labeled with the sampling date (month.year). The bottom-left chart shows seasonal changes in macroalgal diversity, with GpDs calculated from all the dredges associated to each annual season, regardless of the cruise. The bottom-right chart represents four Summer cruises conducted before and after the 2010 Deepwater Horizon oil spill (DWH); dredges launched one year after the DWH (2011: diagonal lines) showed a statistically significant increase in diversity (P-Value <0.05) that ceased the following year (2012). Seasons are indicated with bar colors: White = Spring; Grey = Summer; Black = Fall.

Table 8: Wilcoxon tests P-Values for pairwise differences in macroalgal diversity, measured as F-groups per dredge. P-Values ≤0.05 are highlighted in grey and indicate statistically significant differences between the cruises listed on the corresponding column and row. To fit this table in the document, columns and rows without statistically significant P-Values are not shown.

	Sep.14	Oct.13	Nov.12	Aug.12	Aug.11	Dec.10	Aug.08
Oct.13	0.02						
Nov.12	0.08	0.35					
Aug.12	1.00	0.01	0.05				
Aug.11	0.15	0.00	0.02	0.03			
Dec.10	0.07	0.60	1.00	0.07	0.00		
Aug.08	0.22	0.06	0.54	0.15	0.01	0.38	
Jul.06	0.05	0.01	0.05	0.03	0.05	0.01	0.00
Jun.05	0.05	0.01	0.05	0.03	0.03	0.01	0.00
May.04	0.08	0.02	0.07	0.05	0.18	0.02	0.03
Jun.03	0.53	0.00	0.07	0.36	0.97	0.02	0.03
Jun.01	0.45	0.01	0.04	0.39	0.61	0.01	0.01
May.00	0.36	0.00	0.03	0.16	0.75	0.01	0.02

Table 9: 3-Way Analyses of Similarity performed on the DOMDIS matrix of distance between cruises. Seasons, locations, and the Deepwater Horizon oil spill (before vs. after) were included as fully crossed factors (AxBxC model). Seasons were based on the Unconstrained Divisive Clusters of Ewing Bank. The P-Values for Season and Location are based on 999 permutations whereas the DWH P-Value is based on 336.

	Balata Groups		Semi-Taxa	
Factor	Global-R	P-Value	Global-R	P-Value
Season	0.734	0.001	0.254	0.044
Location	0.707	0.004	0.501	0.002
DWH	0.32	0.196	0.042	0.375
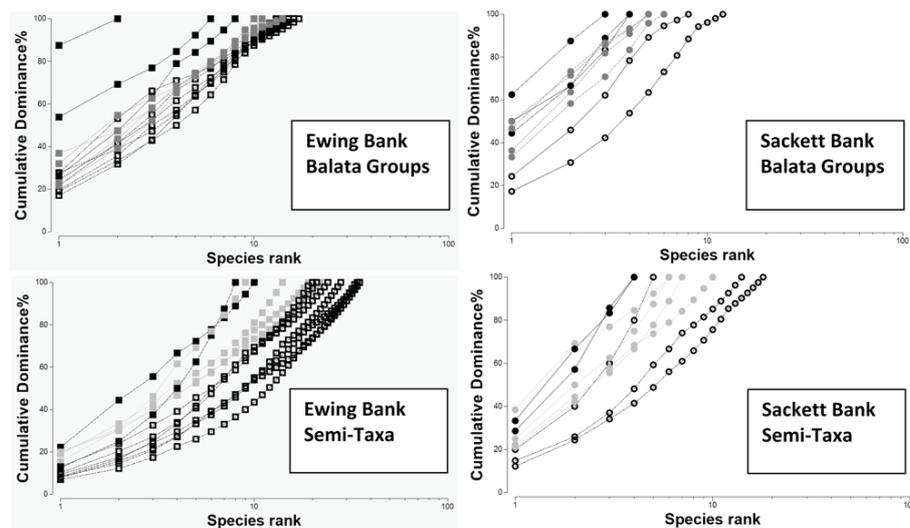
Figure 6: Dominance plots of cruise samples from Ewing and Sackett banks, using Balata Groups and Semi-Taxa. Seasons, based on the Unconstrained Divisive Clusters of Ewing Bank, are indicated with colors. White: Spring; Gray: Summer; Black: Fall.

The seasonal changes of the macroalgal community appear to be a delayed response to environmental factors. For example, whereas the summer environmental conditions occur from July to August, the summer macroalgal community appeared during August and September (Figure 1,2: top). This late response coincides with a delay in the peak of maximum *in situ* temperature, compared with the peak of Surface temperature (Figure 5: right). Whereas surface temperatures reach their maximum values from July to September, the *in situ* temperatures reach their peak from September to November, and then decrease again. This may explain the similarity between the macroalgal assemblages from summer and December, which occur immediately before and after the peak of maximum *in situ* temperature.

Seasonal shifts in macroalgal abundances as well as changes in biodiversity and dominance were more pronounced at Ewing Bank than at Sackett Bank, which is an atypical location that does not follow the community patterns from offshore Louisiana [3]. The unusual divergence of Sackett Bank is probably due to extreme exposure to river discharges since it is located at ca. 50 km south from the Mississippi Delta whereas other offshore banks are located at more than 100 km from any river mouth [3,45]. Therefore, the seasonal structure of Ewing Bank better represents, to a reasonable extent, the typical dynamics of other offshore banks in Louisiana.

Changes in the macroalgal community after the Deepwater Horizon oil spill

Dredge-based One-Way ANOSIMs and nMDS plots showed that the community structure of Ewing Bank changed after the Deepwater Horizon oil spill (DWH) (Table 3, Figure 3). This change was detected only with the summer dredges, which had large sample sizes before and after the DWH. Unfortunately, testing for similar patterns during other seasons was problematic due to small sample sizes. For example, fall dredges were launched only after the DWH whereas spring dredges were launched mostly before the disaster. Conversely, the summer season had more than 15 dredges collected before and after the DWH, respectively.

The differences between red, brown and green seaweed samples collected before vs. after the DWH were stronger for Semi-Taxa than Balata Groups; such differences were mostly contributed by *Anadyomene, Asteromenia, Calonitophyllum, Champia, Dasya, Kallymenia, Lithophyllum, Lithothamnion, Phyllodictyon, Predaea, Pseudocodium,* and *Rhodymenia,* Semi-Taxa which were recorded only before the DWH [2]. Additionally, summer records of *Valonia* and *Halymenia* were observed only after the DWH. Despite the absence of several Semi-Taxa, summer dredges launched after the DWH showed a larger biodiversity due to the presence of other Semi-Taxa that replaced the previous ones.

This rise in macroalgal biodiversity occurred during the first summer post-DWH (August 2011: 9.75 GpD), which showed statistically significant differences (Wilcoxon P-Value <0.05) with a summer cruise performed pre-DWH (August 2008: 4.54 GpD). The biodiversity declined again during the second summer post-DWH (August 2012: 6.38 GpD), showing statistically significant differences with the preceding year but non-significant differences with pre-DWH levels. After 2012, the summer diversity did not vary significantly (Table 8, Figure 6, at bottom-right).

The previous pattern is typical during processes of ecological succession on moderately disturbed substrata, as indicated by a vast amount of literature on the intermediate disturbance hypothesis [46-54]. Specifically, if the DWH cleared significant amounts of substratum but left relatively undisturbed patches, the diversity would increase because species that thrive at both early and late successional stages can coexist after the disaster. However, once the disturbance is removed, biodiversity would decline again as competitive exclusion increases in later successional stages. The moderate ANOSIM R-Values (0.3-0.5) associated with DWH also suggest the existence of an intermediate rather than an acute disturbance.

The results of this study are consistent with the observations of Fredericq et al. [10], who reported the establishment of rich macroalgal communities in successional microcosms consisting of rhodoliths (algal nodules predominantly accreted by crustose coralline algae) and seawater, collected after the DWH, from Ewing and Sackett banks (*in situ* seawater). Fredericq et al. [10,11] revealed the existence of species whose early life-stages (e.g. propagules) occurred in the *in situ* rhodoliths but their adult-stages (i.e. gametophytes, sporophytes) had never been reported in the *in situ* benthos (e.g. *Schmitzia*), and viewed the interior of the rhodoliths as seedbanks for algal community regeneration. Similarly, the results reported here suggest the existence of F-groups that did not typically occur in the benthos, during the summer, until the DWH presumably cleared the substratum, allowing the recruitment of their early-life stages.

The results contrast with the field findings of Fredericq et al. [10,11], Felder et al. [22], Krayesky-Self et al. [28] who reported a strong biodiversity decline in the macroalgal community of Ewing and Sackett banks post-DWH. Such disagreement is particularly interesting since both studies used the same cruise records evaluated here; however, Fredericq et al. [10] and Felder et al. [22] did not consider the existence of seasonal structure when comparing the presence/absence of species before vs. after the DWH. Such an approach can be viewed as problematic because: 1) most cruises conducted before the DWH occurred during the spring (April-July), and 2) most cruises conducted after the DWH occurred during the summer (August-September) and Fall (October-December). Hence, the biodiversity decline and prevalent occurrence of bare rhodoliths reported in Fredericq et al. [10] and Felder et al. [22] may also reflect seasonal differences rather than exclusively DWH effects.

Importantly, the rise in biodiversity reported here should not be understood as a permanent condition resulting from the DWH but rather as a typical community response to a disturbance that may not necessarily be caused by crude oil but by other factors associated with the DWH such as the release of Corexit oil dispersant [19,21]. Fishery closures near the disaster for a prolonged period likely played a part as well since they might temporarily increase the abundance of fishes that graze on macroalgae. Finally, it is possible too that community changes that occurred after 2010 were unrelated to the DWH. Nevertheless, regardless of the causes of this disturbance, the GpD measurements of August 2012 and September 2014 suggest that the macroalgal biodiversity is progressively moving back to pre-DWH levels (Figure 6). On the other hand, the presence/absence of Semi-Taxa appears to be moving far from the pre-DWH level (Figure 4) but this must be verified in future studies of the summer community at Ewing Bank. It is recommended that such studies use sample sizes of at least 15 dredges, to preserve a reasonable statistical power in multivariate analyses.

CONCLUSION

In summary, this study revealed the existence of a strong seasonal structure in the macroalgal communities from offshore Louisiana. Seasonal changes in the overall environmental factors were followed by changes in the macroalgal community, with a one-month delay. This late response coincided with a delay in the peak of maximum *in situ* temperature, compared with the peak of Surface temperature. These results coincided with various studies worldwide (including the NW coast of the Gulf of Mexico) reporting temperature as the main predictor of seasonal structure in macroalgal communities.

This study also found that the community structure of Ewing Bank changed after the Deepwater Horizon oil spill (DWH). These changes were detected in the summer dredges, which had satisfactory sample sizes before and after the DWH. Interestingly, despite the absence of several Semi-Taxa, summer dredges launched after the DWH showed a larger biodiversity due to the presence of other Semi-Taxa that replaced the previous ones.

This rise in biodiversity was statistically significant during 2011 but seems progressively declining towards pre-DWH levels. Conversely, the presence/absence of Semi-Taxa appeared to be moving away, progressively, from the pre-DWH level. This, however, must be verified in future studies of the summer community of Ewing Bank. Finally, it is important to highlight that community changes observed after the DWH may not necessarily be caused by crude oil but instead may have resulted from other factors associated with the disaster or be completely unrelated to the event.

ACKNOWLEDGMENTS

REFERENCES

1. Eiseman NJ, Blair SM. New records and range extensions of deepwater algae from East Flower Garden, northwestern Gulf of Mexico. Contrib Mar Sci. 1982;25:21-26.

2. Fredericq S, Cho TO, Earle SA, Gurgel CF, Krayesky DM, Cid LEM, et al. Seaweeds of the Gulf of Mexico. In: Felder DL, Camp DK (eds) Gulf of Mexico–Origins, waters and biota. Vol 1: Biodiversity. Texas A&M Press, College Station, 2009;187-259.

3. Venera-Pontón DE. Population genetics and ecological structure in macroalgal communities from offshore banks exposed to the Deepwater Horizon oil spill in the NW Gulf of Mexico. Unpublished Doctoral Dissertation, University of Louisiana at Lafayette. 2017;pp:146.

4. Taylor WR. Sketch of the character of the marine algal vegetation of the shores of the Gulf of Mexico. Fish Bull. 1954;55:177-192.

5. Kapraun DF. Seasonal periodicity and spatial distribution of benthic marine algae in Louisiana. Contr Mar Sci. 1974;18:139-167.

6. Kaldy JE, Dunton KH, Czerny AB. Variation in macroalgal species composition and abundance on a rock jetty in the northwest Gulf of Mexico. Bot Mar. 1995;38:519-527.

7. Fredericq S, Gavio B, Phillips N. Observations on the macroalgae inhabiting deep-water hard bank communities in the northwestern Gulf of Mexico. Gulf Mex Sci. 2000;2000:88-96.

8. Rezak R, Bright TJ, McGrail DM. Reefs and banks of the Northwestern Gulf of Mexico: their geological, biological, and physical dynamics. John Wiley & Sons, New York. 1985;pp:259.

9. Gluyas J, Swarbrick R. Petroleum Geoscience. Blackwell Publishing, Malden. 2004; pp:389.

10. Fredericq S, Arakaki N, Camacho O, Gabriel D, Krayesky D, Krayesky SS, et al. A dynamic approach to the study of rhodoliths: a case study for the northwestern Gulf of Mexico. Cryptog Algol. 2014;35(1):77-98.

11. Fredericq S, Self SK, Sauvage T, Richards J, Kittle R, Arakaki N, et al. The critical importance of rhodoliths in the life cycle completion of both macro-and microalgae, and as holobionts for the establishment and maintenance of marine biodiversity. Front Mar Sci. 2019;5:502.

12. Gore RH. The Gulf of Mexico. Sarasota, FL: Pineapple Press. 1992;pp:384.

13. Turner RE, Rabalais NN. The Gulf of Mexico. In: World Seas: An Environmental Evaluation. 2nd Edition. Academic Press. 2018;pp:445-464.

14. Atlas RM, Hazen TC. Oil biodegradation and bioremediation: a tale of the two worst spills in U.S. history. Env Sci Technol. 2011;45(16):6709-6715.

15. Liu Y, Weisberg RH, Hu C, Zheng L. Tracking the Deepwater Horizon oil spill: a modeling perspective. Eos Trans AGU. 2011;92(6):45-46.

16. Barron MG. Ecological impacts of the Deepwater Horizon oil spill: implications for immunotoxicity. Toxicol Pathol. 2012;40(2):315-320.

17. Rabalais N. Assessing early looks at biological responses to the Macondo event. Bioscience. 2014;64(9):757-759.

18. Lehr B, Bristol S, Possolo A. Oil budget calculator: Deepwater Horizon. Washington DC. 2010;pp:217.

19. OSAT. Summary report of sub-sea and sub-surface oil and dispersant detection: sampling and monitoring. Operational Science Advisory Team Report 1, New Orleans. 2010;pp:131.

20. OSAT. Summary report for fate and effects of remnant oil in the beach environment. Operational Science Advisory Team Report 2, New Orleans. 2011;pp:36.

21. Kujawinski EB, Soule MCK, Valentine DL, Boysen AK, Longnecker K, Redmont MC. Fate of dispersants associated with the Deepwater Horizon oil spill. Env Sci Techn. 2011;45:1298-1306.

22. Felder DL, Thoma BP, Schmidt WE, Sauvage T, Krayesky SSL, Chistoserdov A, et al. Seaweeds and decapod crustaceans on gulf deep banks after the Macondo oil spill. Bioscience. 2014;64(9):808-819.

23. Joyce EA, Williams J. Rationale and pertinent data. Mem Hourglass Cruises. 1969;1:11-50.

24. Richards JL, Gabrielson PW, Fredericq S. New insights into the genus *Lithophyllum* (Lithophylloideae, Corallinaceae, Corallinales) from offshore the NW Gulf of Mexico. Phytotaxa. 2014;190:162-175.

25. Richards JL, Pinto TV, Schmidt WE, Sauvage T, Gabrielson PW, Oliveira MC, et al. Molecular and morphological diversity of *Lithothamnion* spp. rhodoliths (Hapalidiaceae, Hapalidiales) from deepwater rhodolith beds in the northwestern Gulf of Mexico. Phytotaxa. 2016;278(2):81-114.

26. Richards JL, Fredericq S. *Sporolithon sinusmexicanum* sp. nov. (Sporolithales, Rhodophyta): a new rhodolith-forming coralline species from deepwater rhodolith beds in the Gulf of Mexico. Phytotaxa. 2018;350:135-146.

27. Sauvage T, Schmidt WE, Suda S, Fredericq S. A metabarcoding framework for facilitated survey of endolithic phototrophs with *tuf*A. BMC Ecol. 2016;16:8.

28. Self SK, Schmidt WE, Phung D, Henry C, Sauvage T, Camacho O, et al. Eukaryotic life inhabits rhodolith-forming coralline algae (Hapalidiales, Rhodophyta), remarkable marine benthic microhabitats. Sci Rep. 2017;1:45850.

29. Schmidt WE, Troche CL, Ballantine DL, Arakaki N, Norris JN, Gabriel D, et al. Taxonomic transfer of *Chrysymenia*

enteromorpha and *C. wrightii* to *Botryocladia* (Rhodymeniaceae, Rhodymeniales, Rhodophyta). Phytotaxa. 2017;324:122-138.

30. Camacho O, Sauvage T, Fredericq S. Taxonomic transfer of *Syringoderma* to *Microzonia* (Syringodermataceae, Syringodermatales), including the new record *M. floridana* (E.C.Henry) comb. nov. in the Gulf of Mexico. Phycologia. 2018;57(4):413-421.

31. Balata D, Piazzi L, Rindi F. Testing a new classification of morphological functional groups of marine macroalgae for the detection of responses to stress. Mar Biol. 2011;158(11):2459-2469.

32. Warwick RM, Clarke KR. Increased variability as a symptom of stress in marine communities. J Exp Mar Biol Ecol. 1993;172(1-2):215-226.

33. Clarke KR, Gorley RN, Somerfield PJ, Warwick RM. Change in marine communities: an approach to statistical analysis and interpretation. Third edition. Primer-E Ltd, Plymouth. 2014;pp:262.

34. Bray RJ, Curtis JT. An ordination of the upland forest communities of southern Wisconsin. Ecol Monogr. 1957;27(4):325-349.

35. Legendre P, Legendre L. Numerical ecology. Third English edition. Elsevier, Amsterdam. 2012;pp:853.

36. Clarke KR, Gorley RN. PRIMER v7: User manual/tutorial. Primer-E Ltd, Plymouth, 2015;PP:300.

37. Boyer TP, Antonov JI, Baranova OK, Coleman C, Garcia HE, Grodsky A, et al. World ocean database 2013. In: Levitus S, Mishonov A (eds) NOAA atlas NESDIS 72, Silver Spring, pp:209.

38. Clarke KR, Somerfield PJ, Gorley RN. Testing of null hypotheses in exploratory community analyses: Similarity profiles and biota-environment linkage. J Exp Mar Biol Ecol. 2008;366(1-2):56-69.

39. Clarke KR, Ainsworth M. A method of linking multivariate community structure to environmental variables. Mar Ecol Prog Ser. 1993;92:205-219.

40. Zar JH. Biostatistical analysis. 5th edition. Pearson-Prentice Hall, Upper Saddle River. 2010;pp:944.

41. Meyer GB. Altas temperaturas estacionales del agua como condición disturbadora de las macroalgas del Parque Nacional Tairona, Caribe Colombiano: una hipótesis. An Inst Invest Mar Punta Betín. 1990;19:9-21.

42. Pulido GD, Ferreira JG. Seasonality in algal assemblages on upwelling-influenced coral reefs in the Colombian Caribbean. Bot Mar. 2002;45(3):284-292.

43. Kim KY, Choi TS, Huh SH, Garbary DJ. Seasonality and community structure of subtidal benthic algae from Daedo Island, southern Korea. Bot Mar. 1998;41:357-365.

44. Espinosa F, García JMG. Algae, macrofaunal assemblages and temperature: a quantitative approach to intertidal ecosystems of Iceland. Helgol Mar Res. 2005;59(4):273-285.

45. Hickerson EL, Schmahl GP, Robart M, Precht WE, Caldow C. The state of coral reef ecosystems of the Flower Garden Banks, Stetson Bank, and other banks in the northwestern Gulf of Mexico. In: The State of Coral Reef Ecosystems of Flower Garden Banks. 2008;190-218.

46. Paine RT, Vadas RL. The effects of grazing by sea urchins, *Strongylocentrotus* spp., on benthic algal populations. Limnol Ocean. 1969;14(5):710-719.

47. Grime JP. Competitive exclusion in herbaceous vegetation. Nature. 1973;242 (5396):344-347.

48. Connell JH. Diversity in tropical rain forests and coral reefs. Science. 1978;199(4335):1302-1310.

49. Huston MA. A general hypothesis of species diversity. Am Nat. 1979;113:81-101.

50. Vandermeer J, D Boucher, I Perfecto, IG de la Cerda A. Theory of disturbance and species diversity: evidence from Nicaragua after Hurricane Joan. Biotropica. 1996;28:600-613.

51. Shea K, Roxburgh SH, Rauschert ESJ. Moving from pattern to process: coexistence mechanisms under intermediate disturbance regimes. Ecol Lett. 2004;7(6):491-508.

52. England PR, Phillips J, Waring JR, Symonds G, Babcock R. Modelling wave-induced disturbance in highly biodiverse marine macroalgal communities: support for the intermediate disturbance hypothesis. Mar Freshw Res. 2008;59(6):515-520.

53. Catford JA, Daehler CC, Murphy HT, Sheppard AW, Hardesty BD, Wescott DA, et al. The intermediate disturbance hypothesis and plant invasions: Implications for species richness and management. Perspect Plant Ecol Evol Syst. 2012;14:231-241.

54. Sheil D, Burslem DFRP. Defining and defending Connell's intermediate disturbance hypothesis: a response to Fox. Trends Ecol Evol. 2013;28(10):571-572.